Achievable Sum Rate Analysis of ZF Receivers in 3D MIMO Systems

Xingwang Li, Lihua Li, and Ling Xie
State Key Laboratory of Networking and Switching Technology, Beijing University of Posts and Telecommunications, No.10, Xitucheng Road, Haidian District, Beijing, China
[E-mail: lixingwangbupt@gmail.com, lilihua@bupt.edu.cn, xieling@bupt.edu.cn]
*Corresponding author: Lihua Li

Received November 11, 2013; revised February 13, 2014; accepted March 25, 2014; published April 29, 2014

Abstract

Three-dimensional multiple-input multiple-output (3D MIMO) and large-scale MIMO are two promising technologies for upcoming high data rate wireless communications, since the inter-user interference can be reduced by exploiting antenna vertical gain and degree of freedom, respectively. In this paper, we derive the achievable sum rate of 3D MIMO systems employing zero-forcing (ZF) receivers, accounting for log-normal shadowing fading, path-loss and antenna gain. In particular, we consider the prevalent log-normal model and propose a novel closed-form lower bound on the achievable sum rate exploiting elevation features. Using the lower bound as a starting point, we pursue the "large-system" analysis and derive a closed-form expression when the number of antennas grows large for fixed average transmit power and fixed total transmit power schemes. We further model a high-building with several floors. Due to the floor height, different floors correspond to different elevation angles. Therefore, the asymptotic achievable sum rate performances for each floor and the whole building considering the elevation features are analyzed and the effects of tilt angle and user distribution for both horizontal and vertical dimensions are discussed. Finally, the relationship between the achievable sum rate and the number of users is investigated and the optimal number of users to maximize the sum rate performance is determined.

Keywords: 3D MIMO, lower bound, Rayleigh fading, large-scale MIMO, achievable sum rate

This paper is funded by the National Science and Technology Major Project (No. 2013ZX03003009), the Creative Research Groups of China (61121001), National 863 Project (No. 2014AA01A705). Authors express our thanks to Prof. Charles Cavalcante as well as the anonymous reviewers for their constructive comments. Prof. Ping Zhang and Dr. Michail Matthaiou are also greatly acknowledged for their guidence and suggestions.

http://dx.doi.org/10.3837/tiis.2014.04.012

1. Introduction

Multiple-input multiple-output (MIMO) technology can provide a remarkable increase in data rate and reliability compared to single-antenna systems. Recently, multiuser MIMO (MU-MIMO) system, where the base station is equipped with multiple antenna elements and simultaneously communicates with several co-channel users, has gained much attention [1] [2] [3]. Currently, most researches on MU-MIMO focus on two-dimensional (2D) channel model, which considers the horizontal dimension only while ignoring the effects of elevation in the vertical dimension. However, the assumption of 2D propagating waves is no longer valid in some circumstances when the elevation spectrum is significant, especially in in-door and in-vehicle environments. To make the channel model more applicable, several studies have taken three-dimensional (3D) MIMO into consideration. In the modeling of 3D MIMO channels, it is well known that the most common and prevalent channel model is the antenna tilting 3D model, which has been extensively used to approximate the propagation in radar and RF communication systems [4] [5] [6]. Literature [7] proposes an approximated 3D antenna radiation pattern that combines the two principal cuts for azimuth (horizontal) and elevation (vertical) planes. The combination in [8] shows a tolerable approximation deviation. In [7], the 3D antenna pattern and approximation are similar to [8] but it assumes that the gains in horizontal and vertical directions are equally weighted, which makes the model more practical and extensively used. Similar approximation is used in this paper as well.

Very recently, there has been a great deal of interest in large-scale MIMO (a.k.a. massive MIMO) systems, where the base station is equipped with a very large number of low power antenna elements, simultaneously serving tens of users [9] [10]. In the context of large-scale MIMO, intracell interference can be substantially reduced with simple linear signal processing [11]. The energy and spectral efficiency, when the number of base station antenna elements grows to very large, are investigated in [12] [13] for maximum-ratio combining (MRC), zero-forcing (ZF) and minimum mean-square error (MMSE) schemes in the uplink. In [14], utilizing tools of random matrix theory, the authors derive deterministic approximations of the uplink SINR with MRC and MMSE receivers, assuming that the numbers of both transmit antenna elements and users grow to infinity for a fixed ratio. They also show that the deterministic approximation of SINR is tight even with a moderate number of base station antenna elements and users. More advantages of massive MIMO are established in [9] [11].

Additionally, user distribution is also an important factor that influences the performance of wireless communication systems. Current literature has paid considerable attention to the uniform distribution, since the uniform user distribution is always adopted for the convenience of mathematical analysis. However, uniform user distribution is not valid in some cases. To make the distribution more general, several papers have investigated the effects of non-uniform user distributions on system performance [15] [16]

[17] [18]. When it comes to the in-building environments such as high-rise residences and office buildings, a large number of potential mobile users are distributed throughout a relatively small 3D space. The users are not only distributed in the single horizontal plane, but also the users have a vertical distribution through different floors. Thus, how to exploit the 3D user distribution to optimize the system performance will be discussed in this paper.

Although a lot of researches on 3D MIMO and large-scale MIMO have appeared, there is no work showing a combination of these two. This paper aims to investigate the performance of ZF receivers considering 3D MIMO and 3D user distribution, as well as the large-scale antenna elements at the base station. To the best of our knowledge, the relevant studies have been reported in [14] [19] [20] [21]. The authors in [19] propose closed-formed bounds on the achievable sum rate and pursue a "large-scale antenna" analysis, while 3D MIMO and user distribution are not considered. On similar grounds, using tools of random matrix theory, [14] [20] derive a deterministic approximation of uplink SINR with linear receivers, assuming that the number of receive antennas and the number of users go to infinity at the same rate. However, since the limiting SINR obtained therein is deterministic, this approximation does not enable further manipulations and consider 3D MIMO and the vertical user distribution. In [21], the authors study the achievable sum rate of 3D MU-MIMO systems and analyze the achievable sum rate performance for different user distributions in high-building with several floors; yet, the final expression is analytical and does not give bounds. More importantly, the highly promising technology of large-scale MIMO system is not investigated. In this paper, we mainly contribute on the achievable sum rate derivation and propose a novel lower bound for the uplink MU-MIMO scenario with 3D MIMO**,** in which 3D user distribution and the "large-scale MIMO" are considered.

The contributions of this paper can be summarized as follows:

(1) We introduce a 3D propagation model with a high-rise building, derive and analyze the achievable sum rate of the single-cell uplink system with 3D MIMO base station and 3D user distribution.

(2) Using the recent generic bounding technique as a starting point [13], we are first to derive the lower bound of the achievable sum rate in closed-form of ZF receivers in 3D MIMO systems. The proposed bound remains relatively tight across the entire SNR and tilt angle ranges.

(3) With the help of the proposed bound, we analyze the asymptotic lower bound for large-scale MIMO systems under the cases of fixed average transmit power and fixed total transmit power. It is shown that the proposed lower bound is applicable for arbitrary number of antennas and remains relatively tight across the entire SNR and tilt angle ranges, whilst the lower bound tightens when the number of antenna elements grows large.

(4) Utilizing the analytical achievable sum rate expression and the lower bound, the optimal number of users to maximize the achievable sum rate of the 2D MIMO and 3D MIMO systems is investigated as well.

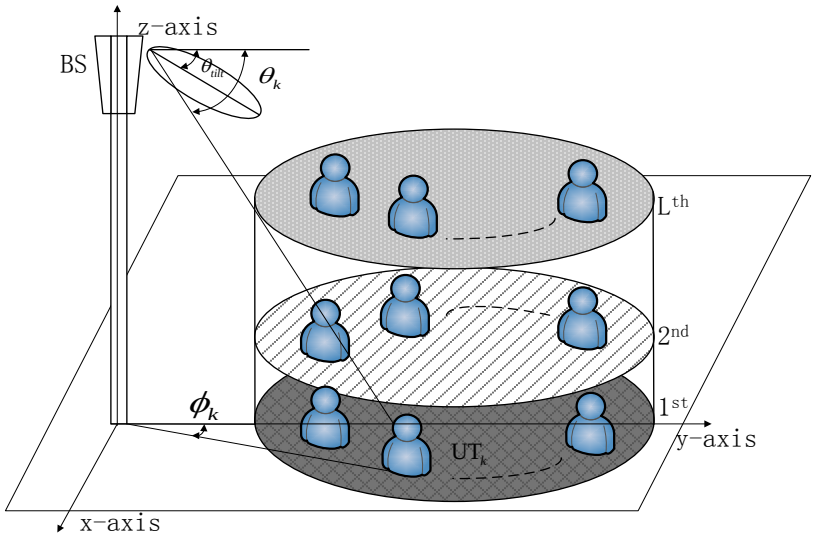

Fig. 1. Schematic illustration of 3D MIMO system with K UTs located in a building with L floors

(5) Antenna tilt angle in the 3D base station is adjusted to achieve the optimal performance. Thus, by exploiting the results of (2), the optimal tilt angle is investigated and the whole performance and the effects of each floor are discussed.

The rest of the paper is organized as follows. Section 2 describes the 3D MIMO fading channel model and the 3D user distribution. In Section 3, we present the derivation of the ergodic achievable sum rate and the lower bound with 3D MIMO base station exploiting variable elevation, while Section 4 elaborates on the achievable sum rate performance of large-scale 3D MIMO topologies. We present some numerical results and corresponding analysis in Section 5 before we conclude the paper in Section 6.

2. 3D MIMO Fading Channel Model and 3D User Distribution

2.1 3D MIMO fading channel model

We consider an uplink 3D MIMO system with N receive antenna elements at the base station and K single-antenna users. It is required that $N \geq K$. All users are located in a building with L floors. We assume that there are K_l users on the l th floor which satisfies the sum of all users in the building is $K = \sum_{l=1}^{L} K_l$. In this paper, floor penetration loss, surface reflection loss**,** and glass penetration loss are not taken into account. A schematic illustration of the multiuser 3D MIMO system under consideration is depicted in **Fig. 1**. Assuming no channel state information (CSI) at the transmitters, the available average power, p_u**,** is identical amongst all users. Thus, the received signal vector $\mathbf{y} \in \mathbb{C}^{N\times 1}$ of the base station is given by

$$\mathbf{y} = \sqrt{p_u}\mathbf{G}\mathbf{x} + \mathbf{n} \tag{1}$$

where $\mathbf{G} \in \mathbb{C}^{N\times K}$ represents the channel matrix between the base station and the K users, i.e., $g_{nk} = [\mathbf{G}]_{nk}$ is the channel coefficient between the n th antenna of the base station and the k th user; $\mathbf{x} \in \mathbb{C}^{K\times 1}$ is the transmitted signal vector by the K users; and $\mathbf{n} \in \mathbb{C}^{N\times 1}$ is the additive white Gaussian noise (AWGN) vector with zero mean and unit covariance.

The channel matrix**,** which models the small-scale and the large-scale fading, can be expressed as

$$\mathbf{G} = \mathbf{H}\boldsymbol{\Omega}^{1/2} \tag{2}$$

where $\mathbf{H} \in \mathbb{C}^{N\times K}$ denotes the small-scale fading and the elements of $\mathbf{H}$ are assumed to be identically and independently distributed (i.i.d.) with zero mean and unit variance; $\boldsymbol{\Omega}$ is a $K \times K$ diagonal matrix, which captures the large-scale fading including distance-dependent path-loss, log-normal shadowing fading**,** and antenna gain between the base station and the K users.

The entries of the diagonal matrix $\boldsymbol{\Omega}$ denote the large-scale fading coefficients, which can be expressed by $\boldsymbol{\Omega} = \mathrm{diag}\{\Omega_k\}_{k=1}^{K} = \mathrm{diag}\left\{\zeta_k a(\phi_k,\theta_k) d_k^{-\upsilon}\right\}_{k=1}^{K}$, where ζ_k, $a(\phi_k,\theta_k)$, d_k^{υ} are shadowing fading coefficient, antenna gain, and distance-dependent path-loss, respectively.

In this paper, we adopt the log-normal shadowing fading model, which is widely accepted in both terrestrial and satellite wireless environments[22]. The probability density function (PDF) of the log-normal fading coefficient ζ_k $k = 1,\cdots,K$ is given by

$$p(\zeta_k) = \frac{\xi}{\zeta_k \sigma_k \sqrt{2\pi}} \exp\left(\frac{\xi \ln \zeta_k - \mu_k}{2\sigma_k^2}\right) \quad ,\zeta_k \geq 0 \tag{3}$$

where $\xi = 10/\ln 10 = 4.3429$, and μ_k (dB) and σ_k (dB) are the mean and the standard deviation of $10\log_{10}(\zeta_k)$, respectively.

The antenna gain $a(\Delta\phi_k, \Delta\theta_k)$ as in [23] is determined by the relative angles between the direct line from the k th user to the base station and the main lobe of the base station antenna elements, both in horizontal (azimuth, $\Delta\phi_k$) and vertical (elevation, $\Delta\theta_k$) directions. $(x_{\mathrm{BS}}, y_{\mathrm{BS}}, z_{\mathrm{BS}})$ and (x_k, y_k, z_k) denote the coordinates of the base station and the k th user. The difference of x-coordinate between the k th user and the base station can be expressed by $\Delta x_k = x_k - x_{\mathrm{BS}}$. Similarly, we can obtain Δy_k and Δz_k. With the fixed orientation angle α_{orn}, the relative angles can be calculated as

$$\Delta\phi_k = \mathrm{atan2}(\Delta y_k, \Delta x_k) - \alpha_{\mathrm{orn}} \tag{4}$$

$$\Delta\theta_k = \mathrm{atan2}\left(\Delta \mathrm{z}_k, \sqrt{(\Delta x_k)^2 + (\Delta \mathrm{y}_k)^2}\right) - \beta_{\mathrm{tilt}} \tag{5}$$

where β_{tilt} denotes the antenna tilt angle, $-90^\circ \leq \beta_{\mathrm{tilt}} \leq 90^\circ$.

The antenna gain $a(\Delta\phi_k, \Delta\theta_k)$ can be expressed as follows (the values of horizontal and vertical antenna gains are expressed in decibel)

$$a(\Delta\phi_k, \Delta\theta_k) = -\min\left(\min\left[12\left(\frac{\phi_k - \alpha_{\text{orn}}}{\phi_{\text{3dB}}} \right)^2, SLL_h \right] + \min\left[12\left(\frac{\theta_k - \beta_{\text{tilt}}}{\theta_{\text{3dB}}} \right)^2, SLL_v \right], SLL_{\text{tot}} \right) + a_{\max} \tag{6}$$

where ϕ_{3dB} and θ_{3dB} denote the half-power beam-width (HPBW) in the azimuth and the elevation pattern respectively. SLL_h and SLL_v are the side lobe levels for the azimuth and elevation beams. SLL_{tot} represents the total side lobe level. Finally, $a_{\max}$ indicates the maximum antenna gain.

The distance between the k th user and the base station is denoted by d_k, which can be expressed as

$$d_k = \sqrt{(\Delta x_k)^2 + (\Delta y_k)^2 + (\Delta z_k)^2} \tag{7}$$

With the log-normal shadowing fading coefficient ζ_k, antenna gain $a(\Delta\phi_k, \Delta\theta_k)$ and distance-dependent path-loss $d_k^{-\upsilon}$, we can obtain the large-scale fading coefficient as follows

$$\Omega_k = \zeta_k 10^{\frac{a(\Delta\phi_k, \Delta\theta_k)}{10}} d_k^{-\upsilon} \tag{8}$$

where υ is the path-loss exponent.

All these model parameters are obtained based on the practical antenna Kathrein 742215, which is a commonly deployed antenna and has been widely used in system performance evaluation.

2.2 3D User Distribution Models

In practice, the performance of MIMO systems is affected not only by the fading but also by the user distributions [15] [16] [17] [18]. In the following, we consider the spatial user distribution in the building, which consists of both horizontal plane for each floor and vertical plane for users in different floors. It is assumed that all floors of the building model are circles and have the same radius r.

For horizontal plane, we consider two kinds of user distributions: uniform distribution and Gaussian distribution. For the uniform distribution, we assume that the building shape is approximated by a circle with radius r, and all users (desired and interfering users) are assumed to be independently and uniformly distributed on the circular floor. The typical cases are dormitories and residential buildings. The corresponding probability density function (PDF) can be modeled as follows

$$f(x) = 2x/r^2, \quad 0 \le x \le r \tag{9}$$

As to Gaussian distribution, most users are concentrated in the center of the floor and the density of users along the radius tends to be a Gaussian curve. Typical scenes are "hot-spots" such as city centers, shopping malls, and office areas, etc. The corresponding PDF can be modeled as follows

$$f(x) = \frac{\Delta}{\sigma\sqrt{2\pi}} \exp\left(\frac{-x^2}{2\sigma^2}\right), \quad 0 \le x \le r \tag{10}$$

where σ is the variance and Δ is a constant.

For vertical plane, it is modeled that users on different floors obey some rules. Unlike the horizontal distribution, the vertical distribution is discrete. We hereafter focus on the uniform and exponential distributions. Uniform vertical distribution means that the number of users on each floor is equal. This is a common scenario in real life such as dormitories and residential buildings, where for all floors, the numbers of rooms and users in a room are relative certain and approximately equal. Thus, the corresponding probability mass function (PMF) can be given by

$$g(l) = \begin{cases} c, & l = 1, 2, \cdots, L \\ 0 & others \end{cases} \tag{11}$$

where l is the index of the floor, and c indicates the number of users that are located on each floor, which is equal for all floors. Exponential vertical distribution means that there are more users on some floors. This is quite common in current life. A shopping mall with a densely populated supermarket on certain floor is one of the cases. The PMF can be obtained as follows

$$g(l) = \begin{cases} \Lambda \Upsilon^{l-1}, & l = 1, 2, \cdots, L \\ 0, & others \end{cases} \tag{12}$$

where l represents the index of the floor, and Υ^l $(0 \le \Upsilon \le 1)$ denotes the ratio between the number of the l th floor's users and the whole building. c and Λ are constants to satisfy that the sum of all users on all floors in the building is K, which is given by

$$K = \sum_{l=1}^{L} g(l) \tag{13}$$

where K denotes the number of users of the whole building.

3. Achievable sum rate and lower bound in 3D MIMO systems

In this section, we focus on the achievable sum rate derivation of the 3D MIMO system. Capitalizing on the results of [13], a novel closed-form bound on the achievable sum rate of 3D MIMO ZF receivers that applies for arbitrary number of antenna and SNR is presented.

3.1 Achievable sum rate in 3D MIMO systems

Assuming that the base station has perfect CSI, which is reasonable in an environment with low or moderate mobility, long training intervals can be afforded. By using the linear detector, the received signal $\mathbf{y}$ is processed by multiplying it with $\mathbf{T}^{\mathrm{H}}$ as follows

$$\mathbf{r} = \mathbf{T}^{\mathrm{H}}\mathbf{y} \tag{14}$$

From (1) and (14), the receive vector after using the linear detector is given by

$$\mathbf{r} = \sqrt{p_u}\mathbf{T}^{\mathrm{H}}\mathbf{G}\mathbf{x} + \mathbf{T}^{\mathrm{H}}\mathbf{n} \tag{15}$$

Let r_k and x_k be the k th elements of the $K \times 1$ vectors $\mathbf{r}$ and $\mathbf{x}$, respectively. Then

$$r_k = \sqrt{p_u}\mathbf{t}_k^{\mathrm{H}}\mathbf{G}\mathbf{x} + \mathbf{t}_k^{\mathrm{H}}\mathbf{n} = \sqrt{p_u}\mathbf{t}_k^{\mathrm{H}}\mathbf{g}_k x_k + \sqrt{p_u}\sum_{i=1,i\neq k}^{K}\mathbf{t}_k^{\mathrm{H}}\mathbf{g}_i x_i + \mathbf{t}_k^{\mathrm{H}}\mathbf{n} \tag{16}$$

where $\mathbf{t}_k$ and $\mathbf{g}_k$ denote the k th columns of detector matrices $\mathbf{T}$ and $\mathbf{G}$, respectively. The output consists of two components: (a) the desired signal component $\sqrt{p_u}\mathbf{t}_k^{\mathrm{H}}\mathbf{g}_k x_k$ and (b) the interference-plus-noise $\sqrt{p_u}\sum_{i=1,i\neq k}^{K}\mathbf{t}_k^{\mathrm{H}}\mathbf{g}_i x_i + \mathbf{t}_k^{\mathrm{H}}\mathbf{n}$. Thus the SINR of the uplink transmission from the k th user to the base station is defined as

$$\gamma_k = \frac{p_u\left|\mathbf{t}_k^{\mathrm{H}}\mathbf{g}_k\right|^2}{p_u\sum_{i=1,i\neq k}^{K}\left|\mathbf{t}_k^{\mathrm{H}}\mathbf{g}_i\right|^2 + \left\|\mathbf{t}_k^{\mathrm{H}}\right\|^2} \tag{17}$$

When using ZF detector, $\mathbf{T}^{\mathrm{H}} = \left(\mathbf{G}^{\mathrm{H}}\mathbf{G}\right)^{-1}\mathbf{G}^{\mathrm{H}}$, or $\mathbf{T}^{\mathrm{H}}\mathbf{G} = \mathbf{I}_K$. Therefore, $\mathbf{t}_k^{\mathrm{H}}\mathbf{g}_i = \delta_{ki}$, where $\delta_{ki} = 1$ when $k = i$ and 0 otherwise. Therefore, the instantaneous received SINR at the k th ZF output is

$$\gamma_k = \frac{p_u}{\left[\left(\mathbf{G}^{\mathrm{H}}\mathbf{G}\right)^{-1}\right]_{kk}} = \frac{p_u\left[\mathbf{\Omega}\right]_{kk}}{\left[\left(\mathbf{H}^{\mathrm{H}}\mathbf{H}\right)^{-1}\right]_{kk}} \tag{18}$$

where $[\cdot]_{kk}$ returns the k th diagonal element of a matrix. The achievable sum rate, assuming independent decoding at the receiver, is essentially the sum of throughputs contributed from all users

$$R = \sum_{k=1}^{K}\mathrm{E}\left[\log_2\left(1+\gamma_k\right)\right] \tag{19}$$

where the expectation is taken over all channel realizations of **G** and the channel is assumed to be ergodic. Clearly, the sum rate analysis of MIMO ZF receivers requires precise knowledge of the statistics of γ_k.

3.2 Closed-form lower bound on the sum rate

Capitalizing on the results of [13], we derive a novel closed-form lower bound on the achievable sum rate of ZF receivers with 3D MIMO that applies for any number of receive antennas and arbitrary SNR.

In the following, we propose the lower bound for Rayleigh/log-normal 3D MIMO channel.

Theorem 1: The achievable sum rate of ZF receivers over Rayleigh/log-normal 3D MIMO channels is lower bounded by

$$R \geq R_L = \sum_{k=1}^{K} \log_2 \left(1 + p_u \left(N - K \right) \exp\left(\frac{\mu_k}{\xi} + \frac{\sigma_k^2}{2\xi^2} \right) 10^{\frac{a\left(\Delta\phi_k, \Delta\theta_k\right)}{10}} d_k^{-\upsilon} \right) \tag{20}$$

Proof: From Eq. (18) and (19), we can obtain the following lower bound on the achievable sum rate

$$\begin{aligned} R \geq R_L &\overset{(a)}{=} \sum_{k=1}^{K} \log_2 \left(1 + \frac{p_u \mathrm{E}\left(\zeta_k 10^{\frac{a\left(\Delta\phi_k, \Delta\theta_k\right)}{10}} d_k^{-\upsilon} \right)}{\mathrm{E}\left\{ \left[\left(\mathbf{H}^H \mathbf{H} \right)^{-1} \right]_{kk} \right\}} \right) \\ &\overset{(b)}{=} \sum_{k=1}^{K} \log_2 \left(1 + \frac{p_u \mathrm{E}\left(\zeta_k 10^{\frac{a\left(\Delta\phi_k, \Delta\theta_k\right)}{10}} d_k^{-\upsilon} \right)}{\frac{1}{K} \sum_{k=1}^{K} \mathrm{E}\left(\left[\left(\mathbf{H}^H \mathbf{H} \right)^{-1} \right]_{kk} \right)} \right) \\ &\overset{(c)}{=} \sum_{k=1}^{K} \log_2 \left(1 + \frac{p_u \mathrm{E}\left(\zeta_k 10^{\frac{a\left(\Delta\phi_k, \Delta\theta_k\right)}{10}} d_k^{-\upsilon} \right)}{\frac{1}{K} \mathrm{E}\left[\mathrm{tr}\left(\left(\mathbf{H}^H \mathbf{H} \right)^{-1} \right) \right]} \right) \end{aligned} \tag{21}$$

where (a) are the results of Eq.(8) and Jensen's inequality since $\log(\cdot)$ is a concave function, (b) and (c) are obtained by using the property of the matrix trace.

With the aid of the following identity [24, Eq. (2.9)],

$$\mathrm{E}\left[\mathrm{tr}\left\{ \mathbf{W}^{-1} \right\} \right] = \frac{m}{n-m} \tag{22}$$

where $\mathbf{W} \sim W_m\left(n, \mathbf{I}_n\right)$ is an $m \times m$ central complex Wishart matrix with n ($n > m$) degrees of freedom**.** Substituting Eq. (22) into Eq. (21), we obtain

$$
\begin{aligned}
R_L &\overset{(d)}{=} \sum_{k=1}^{K} \log_2 \left(1 + \frac{p_u \left(\mathrm{E}\left(\zeta_k 10^{\frac{a(\Delta\phi_k, \Delta\theta_k)}{10}} d_k^{-\upsilon} \right) \right)}{\frac{1}{K}\left(\frac{K}{N-K} \right)} \right) \\
&\overset{(e)}{=} \sum_{k=1}^{K} \log_2 \left(1 + p_u (N-K) \left(\mathrm{E}(\zeta_k) \mathrm{E}\left(10^{\frac{a(\Delta\phi_k, \Delta\theta_k)}{10}} \right) \mathrm{E}\left(d_k^{-\upsilon} \right) \right) \right) \\
&\overset{(f)}{=} \sum_{k=1}^{K} \log_2 \left(1 + p_u (N-K) \left(10^{\frac{a(\Delta\phi_k, \Delta\theta_k)}{10}} d_k^{-\upsilon} \mathrm{E}(\zeta_k) \right) \right)
\end{aligned} \tag{23}
$$

where (d) is obtained by using the formula of Eq. (22), and (e) is obtained by using the property of independence among ζ_k, $d_k^{-\upsilon}$, and $10^{a(\Delta\phi_k, \Delta\theta_k)/10}$ while (f) is obtained by using the determinacy of the coefficients ζ_k and $d_k^{-\upsilon}$.

Finally, for the shadowing terms, recall the fundamental properties of a log-normal variate $\zeta_k \backsim LN\left(\frac{\mu_k}{\xi}, \frac{\sigma_k^2}{\xi} \right)$ [22, Eq. (2.55)]

$$
\mathrm{E}\left[\zeta_k^r \right] = \exp\left(\frac{r}{\xi} \mu_k + \frac{1}{2} \left(\frac{r}{\xi} \right)^2 \sigma_k^2 \right) \tag{24}
$$

Substituting Eq. (24) into Eq. (23) and simplifying the equation, we can conclude the proof.

4. Achievable Sum Rate Analysis of Large-Scale 3D MIMO System with ZF Receivers

Recently, there has been increasing research interest in the area of large-scale MIMO systems, which promises to provide significant power saving and maintain high quality-of-service by deploying hundreds of low-power antenna elements at the base station. However, the impact of 3D MIMO on the sum rate performance in large-scale MIMO systems with linear ZF receivers has seldom been investigated yet. The main goal of this section hereafter is to study how the sum rate of 3D MIMO ZF receivers behaves in the "large-antenna" limit.

In order to obtain some extra insights into the large-antenna analysis, we consider two separate cases:

1) Fixed p_u, K, and $N \to \infty$: Intuitively, when the number of the base station antenna elements grows to infinity, whilst p_u and K are kept fixed, the receiver captures more power without bound. From the lower bound in Eq. (20), as $N \to \infty$, we obtain

$$R_L = \sum_{k=1}^{K} \log_2 \left(1 + p_u \left(N - K \right) \exp\left(\frac{\mu_k}{\xi} + \frac{\sigma_k^2}{2\xi^2} \right) 10^{\frac{a(\Delta\phi_k, \Delta\theta_k)}{10}} d_k^{-\upsilon} \right) \xrightarrow{a.s} \infty \tag{25}$$

From Eq. (25), we can observe that with a large number of receiver antenna elements, the effect of small-scale Rayleigh fading is average out, and R_L is dominated by the number of the base station antenna elements, the mean μ_k and the variance σ_k^2 parameters of shadowing fading, the antenna gain $a(\Delta\phi_k, \Delta\theta_k)$, and the path-loss $d_k^{-\upsilon}$. This means that large-scale MIMO always has the benefit of eliminating the effects of the small-scale and the large-scale fading. Therefore, by increasing N, the sum rate grows without limit.

2) Fixed E_u, K, and $N \to \infty$, let $p_u = E_u / N$: In the context of large-scale antenna systems, the available transmit power should be normalized by the large number of antenna elements at the base station. With the aid of this normalization, we guarantee that the total received power does not diverge as $N \to \infty$. This aspect is very interesting in practice, since it is vital not only from a business point of view but also to address environmental and health concerns. From Eq. (20), we have

$$\begin{aligned} R_L &= \sum_{k=1}^{K} \log_2 \left(1 + \frac{E_u}{N} \left(N - K \right) \exp\left(\frac{\mu_k}{\xi} + \frac{\sigma_k^2}{2\xi^2} \right) 10^{\frac{a(\Delta\phi_k, \Delta\theta_k)}{10}} d_k^{-\upsilon} \right) \\ &\xrightarrow{a.s.} \sum_{k=1}^{K} \log_2 \left(1 + E_u \exp\left(\frac{\mu_k}{\xi} + \frac{\sigma_k^2}{2\xi^2} \right) 10^{\frac{a(\Delta\phi_k, \Delta\theta_k)}{10}} d_k^{-\upsilon} \right), \quad N \to \infty \end{aligned} \tag{26}$$

This result shows that by using a large antenna array at the base station, the transmit power at each user will be cut proportionally to $1/N$ while maintaining a desired quality-of-service (QoS). We can see from Eq. (26) that when the number of the base station antennas grows without limit, the sum rate increases while converges to a deterministic constant. More importantly, even by scaling down the transmit power to $1/N$, the effects of fading still can be averaged out. Finally, we observe that the sum rate increases linearly with the number of active users and logarithmically with the normalized SNR when the number of antennas tends toward infinity.

The purpose of the paper is to derive and analyze the sum rate performance of 3D MIMO and propose a novel lower bound. The impacts of horizontal and vertical user distributions on the sum rate are also analyzed. Using the lower bound as a starting point, we pursue a large-system analysis and provide asymptotic expressions when the number of antennas at the base station grows to infinity. In particular, we study the optimal tilt angle and the optimal number of users to maximize the performance of the building. This is very interesting in practical scenarios, which can be used as a reference for infrastructure.

5. Numerical Results

In the simulation, we assume that the floor penetration loss, surface reflection loss and glass penetration loss are not taken into account. Some numerical results are provided to

verify our analysis. Firstly, we consider a simple scenario where there is only one floor ($L=1$). This setting enables us to validate the accuracy of our proposal lower bound for 3D MIMO and pursue large-system analysis. The fundamental effects of the number of the base station antennas and transmit power of each user are also studied. We then consider a more practical scenario that accounts for horizontal and vertical user distributions for the building with L ($L=3$) floors. The channel incorporates small-scale fading as well as large-scale fading including path-loss, log-normal shadowing fading and antenna gain. In all simulations, we set the parameters of shadowing fading $\mu_k = 4\text{dB}$ and $\sigma_k = 2\text{dB}$, $k=1,2,\cdots,K$, and assume maximal antenna gain and path-loss exponent $\upsilon = 4$. The distance between the base station and the center of the building is D. Tilt angles are given with respect to the ground and positive values mean downward tilting. The 3D MIMO antenna parameters are the same as [23] and given in **Table 1**.

Table 1. 3D MIMO parameters

Class	Value	Class	Value
ϕ_{3dB}	70°	θ_{3dB}	7°
SLL_h	25dB	SLL_v	20dB
SLL_{tol}	25dB	$a_{\max}$	0dBi
$a_{\max}$	70°	α_{orn}	0°

In the following, we investigate six different schemes: (1) sum rate and lower bound corresponding to 2D MIMO and 3D MIMO systems; (2) sum rate via adjusting the tilt angle; (3) large-scale 3D MIMO analysis for fixed average transmit power and fixed total transmit power ;(4) sum rate with different number of users; (5) sum rate performance of each floor and the whole building. (6) impacts of 3D user distribution on the performance of the systems.

5.1 Scenario 1

In this scenario, we consider the uplink of a single cell MU-MIMO system, and all users are located in a building on one floor. The distance between the base station and the center of the building D is set to 1000 m. We assume that all users are uniformly distributed on the floor.

We first investigate the sum rate performance of the proposed lower bound with different tilt angles. In this configuration, $K=2$ users are uniformly distributed on the floor, and the base station is equipped with $N=10$ antenna elements. The radius of the floor in this scenario is set to 100 m.

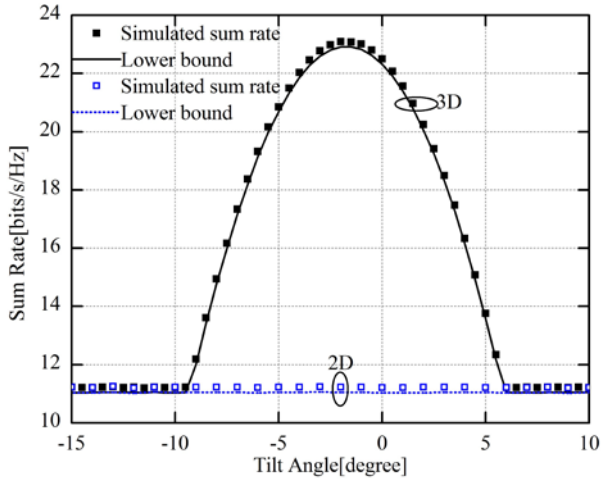

Fig. 2. Simulated sum rate and lower bounds with 2D and 3D MIMO versus tilt angle β_{tilt} ($N = 10$, $K = 2$, $p_u = 5$ dB , $\upsilon = 4$, $\mu = 4$ dB , $\sigma = 2$ dB , D=1000 m)

Fig. 2 shows the sum rates (19) and the exact lower bounds (20) for 2D MIMO and 3D MIMO versus the base station tilt angle. We observe that due to the effect of the vertical antenna gain, 3D MIMO system has a better performance than 2D MIMO system in the tilt range from -9.5° to 6°. The sum rate increases with the tilt angle before the base station is directed to the users and then decreases with the further increase since the radiation angle of the base station antenna deviates from the users. Moreover, the lower bounds of 2D MIMO and 3D MIMO remain tight across the entire tilt angle range. Finally, we can observe that, even for small number of receive antenna elements, the lower bound based on Theorem 1 is sufficiently accurate.

We then assess the sum rate performance of the proposed exact lower bound in (20) versus different transmit power. In **Fig. 3**, we examine the tightness of the lower bound against the SNR. We assume that $K = 2$ and the base station is equipped with $N = 10$ and 50 antenna elements respectively.

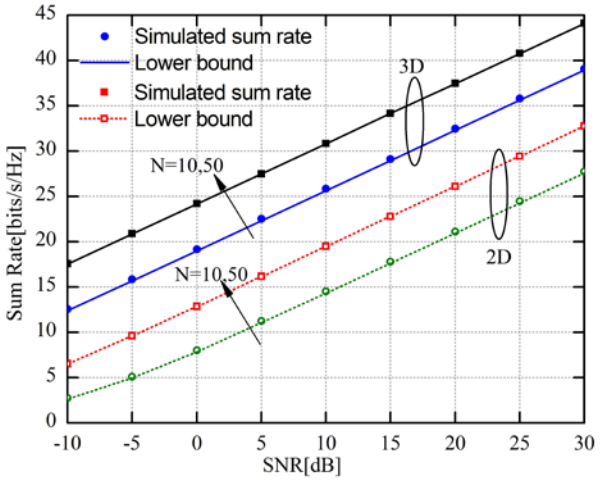

Fig. 3. Simulated sum rate and lower bounds with 2D MIMO and 3D MIMO against the SNR p_u ($K = 2$, $p_u = 10$ dB , $\upsilon = 4$, $\mu = 4$ dB , $\sigma = 2$ dB , D=1000 m)

Clearly, the lower bound R_L tightens (i.e. it closely approaches the exact sum rate curves) at all SNRs and when the number of antennas grows large. At high SNRs, the system is bandwidth limited, thus the sum rate scales linearly with the minimum number of antennas and the bound tightens sufficiently. Besides, the lower bound grows tighter when the number of base station antennas grows from 10 to 50. From **Fig. 3**, we further observe that for all SNRs and numbers of base station antenna $N (N = 10,50)$, the sum rate performance for 3D MIMO outperforms 2D MIMO. Therefore, we can conclude that 3D MIMO predicts the real channel environments more clearly than 2D MIMO.

The sum rate performances of large-scale MIMO systems for 2D MIMO and 3D MIMO are investigated in **Fig. 4** and **Fig. 5**. **Fig. 4** shows the sum rate performance and lower bound in (25) versus N for the case of $p_u = 10$ dB , and **Fig. 5** shows the lower bound in (26) and its asymptote in (26) for the case of $p_u = 10/N$ dB .

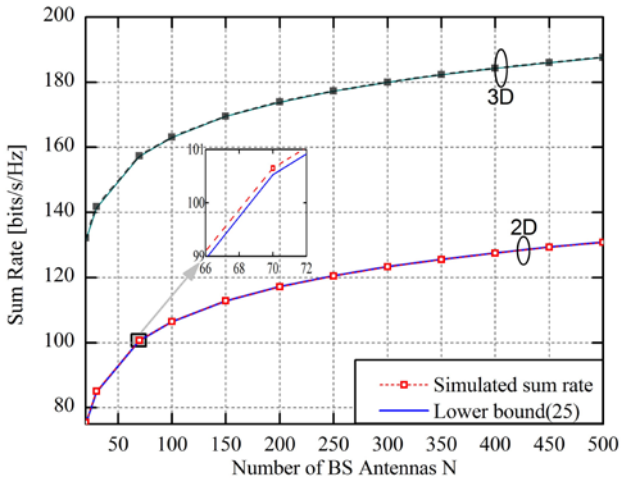

Fig. 4. Simulated sum rate and lower bounds (exact and asymptotic) versus the number of base station antennas N ($K=2$, $p_u=10$ dB, $\upsilon=4$, $\mu=4$ dB, $\sigma=2$ dB, D=1000 m)

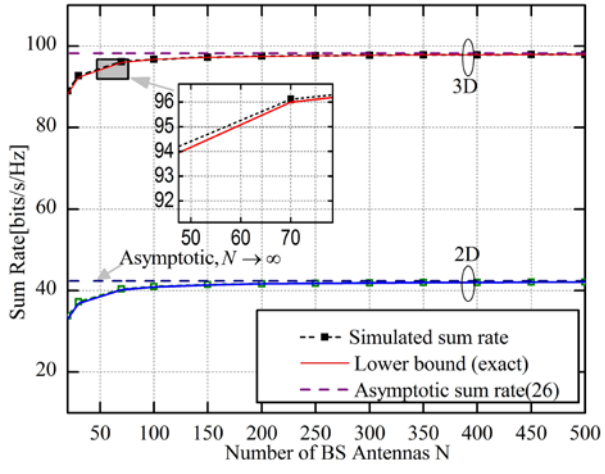

Fig. 5. Simulated sum rate and lower bounds (exact and asymptotic) versus the number of base station antenna N ($K=2$, $p_u=10/N$ dB, $\upsilon=4$, $\mu=4$ dB, $\sigma=2$ dB, D=1000 m)

Fig. 4 and **Fig. 5** exhibit sum rate performances of the proposed lower bound for large array systems for the case $p_u=10$ dB and $p_u=10/N$ dB. As expected, with $p_u=10$ dB, the sum rate grows without bound (logarithmically increasing with the number of the base

station antennas N) when N grows, and with $p_u = 10/N$ dB , the sum rate increases very slowly and converges to a deterministic constant when N increases, which verifies our theoretical analysis. For larger N , the simulated sum rate (short dashed line) and the lower bound (solid line) approach to the asymptotic sum rate (dash line). Moreover, the two figures show that the lower bound R_L remains sufficiently tight across the entire number range of receive antennas, and the sum rate performance for 3D MIMO outperforms 2D MIMO. **Fig. 5** shows that the sum rate converges very fast to the deterministic asymptote, even for a moderate number of receive antennas.

Fig. 6 shows the sum rate performance versus different number of users for 2D MIMO and 3D MIMO at $N = 20$ under the cases of $p_u = 10$ dB and $p_u = 10/N$ dB.

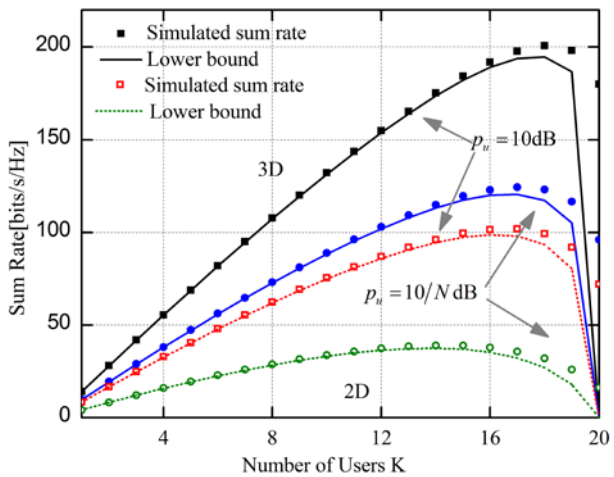

Fig. 6. Simulated sum rate and lower bound of the whole building versus the number of users K ($N = 20$, $\upsilon = 4$, $\mu = 4$ dB , $\sigma = 2$ dB , D=1000 m)

From **Fig. 6**, it can be observed that for small K , the sum rate is intuitively small. For the largest number of users ($K = N$), the sum rate is also small because that the more users are served, the less transmit dimensions for each user is left. Therefore, it indicates that it is not optimal anymore to serve the maximum number of users. In this figure, we can see that the value of $K = 18,17,16,15$ corresponds to the optimal sum rate performance for 3D/2D MIMO and $p_u = 10\text{dB}$ / $p_u = 10/N$ dB . Moreover, for $M > K + 1$, the lower bound does fit well with the simulated sum rate. This is consistent with the results in [11] [17].

5.2 Scenario 2

In order to get some additional insights into the effects of 3D user distribution on the achievable sum rate, we consider a single-cell MU-MIMO system with a building of

L floors. We assume that all users are located in a building with $L = 3$ floors in which the floor is simplified as a circle with radius $r = 50$ m, as depicted in **Fig.1**. The base station with a height of 30 m is equipped with N antenna elements, and the distance between the base station and the center of the building D is set to 100 m. The storey height is set to 5 m.

First, we analyze the sum rate of the building with different tilt angles for the normal and the uniform horizontal distribution. Only uniform distribution is considered for the vertical dimension. In detail, K ($K = 39$) users are uniformly distributed on the three floors, and each floor has the same number of 13 users. We choose the number of the base station antennas $N = 45$ and 60 respectively.

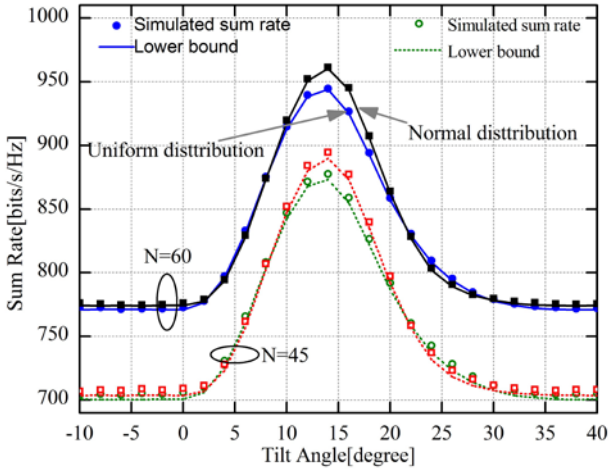

Fig. 7. Simulated sum rate and lower bound of the whole building versus tilt angle considering uniform and normal distribution ($K = 39$, $p_u = 5$ dB, $\upsilon = 4$, $\mu = 4$ dB, $\sigma = 2$ dB, D=100 m)

In **Fig. 7**, we observe that for the uniform and the normal distributions, the sum rates increase with tilt angle before the optimal tilt angle (about 15°) because more users can be served by the vertical antenna pattern. Comparing the curves of normal and uniform distributions, it is not difficult to find a similar global trend for the sum rates, whilst we see that near the optimal tilt angle the performance of normal distribution outperforms the uniform one. Deviating from the optimal tilt angle by about 5°, similar performances are presented for both uniform and normal distributions. Interestingly, for the curves of $N = 45$ and $N = 60$, it is not difficult to observe that a larger N ($N = 60$) makes the lower bound tighter than lower one (N=45). This implies that the large number of receive antennas seems to become sufficiently tight for entire tilt angle ranges. This result is similar to **Fig. 2**, **Fig. 3**, **Fig.4** and **Fig.5**.

The sum rates for each floor are investigated in **Fig. 8**. Again, the lower bound is very tight even for small difference between the number of users K and the number of the base station antennas N . The black, blue and red solid lines and symbols correspond to the case of the normal distribution, while the olive, purple and dark yellow short dot lines and hollow symbol denote the uniform distribution. The optimal sum rates of the two distributions increase from the first floor to the third floor due to the distances between the base station and the users. As anticipated, users on the first floor achieve the smallest optimal sum rate due to the strongest path-loss effect, while on the contrary, users on the third floor achieve the largest optimal sum rate. Furthermore, we observe that the normal distribution performance outperforms the uniform one. This is because for small distance the elevation angle varies faster for different users and different floors. Besides, more users point to the direction of the base station radiation for the normal distribution.

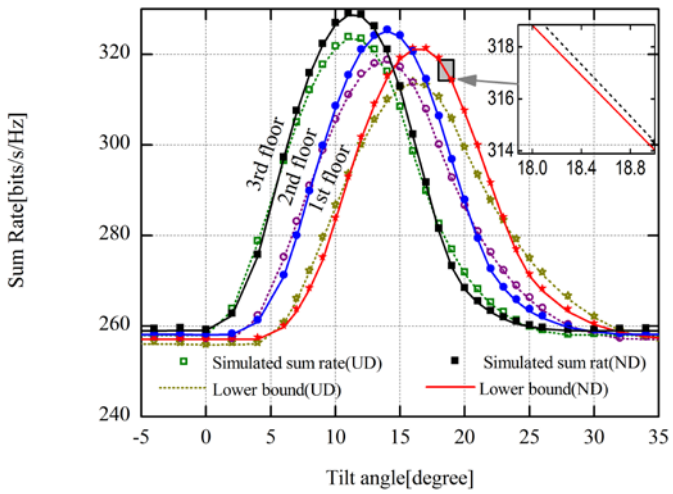

Fig. 8 Simulated sum rate and lower bound of each floor versus tilt angle considering uniform and exponent distribution ($N = 60$, $K = 39$, $p_u = 5$ dB , $\upsilon = 4$, $\mu = 4$ dB , $\sigma = 2$ dB , D=100 m ,UD-uniform distribution, ND-normal distribution)

In the following, the effect of vertical user distribution is studied. The parameters are the same as in **Fig. 6**, except that the users are not uniformly distributed on the three floors. For the convenience of comparison, we consider two vertical user distributions. One is uniform distribution, which serves as a basis of comparison while the other is exponential distribution defined in (12), in which $\Lambda = 27$, $\Upsilon = 1/3$. For the exponential distribution, There are 27, 9, 3 users from the first to the third floor, respectively. Besides, the horizontal user distribution is set to the uniform one. The sum rate considering vertical user distribution is illustrated in **Fig. 9**.

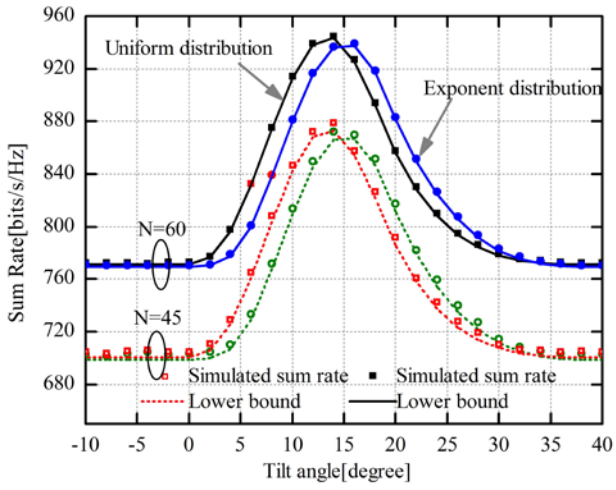

Fig. 9. Simulated sum rate and lower bound versus tilt angle considering uniform and exponent distributions ($K = 39$, $p_u = 5$ dB , $\upsilon = 4$, $\mu_k = 3$ dB , $\sigma_k = 2$ dB , D=100 m)

Fig. 9 shows that the two distributions have a similar global trend, and the sum rate achieves the best performance when the tilt angle is about 15°, which is known as the optimal angle. When the tilt angle deviates from the optimal angle, the sum rate drops dramatically. Furthermore, when the angle is between 0° and 15°, the sum rate for uniform distribution (black and red curves) is larger than exponential distribution (blue and olive curves). However, for the angle between 15° and 35°, the performance of exponential distribution outperforms the uniform distribution. This is because for exponential distribution most users are located on the first floor which has a larger tilt angle. Finally, we observe that the lower bound for $N = 60$ is tighter than $N = 45$, and the lower bound R_L remains relatively tight across the entire tilt angle range. This coincides with the results of [13] [14].

6. Conclusion

This paper mainly focuses on the achievable sum rate performance of 3D MIMO ZF receivers utilizing the antenna tilt angle. In particular, a novel and simple closed-form lower bound is derived, which applies for arbitrary number of antenna elements considering 3D MIMO and 3D user distribution and demonstrates that the sum rates remain tight across the entire SNR and tilt angle ranges. We also examine the emerging area of large-scale MIMO systems in detail and the interesting result that in the "large-system" regime, the lower bound tightens as well is observed. In parallel, we investigate the impacts

of antenna tilt angle on the sum rate both for the whole building and a single floor. We find that the appropriate tilt angle can compensate for the sum rate gain lost in the distance-dependent path-loss. Besides, the optimal number of users to maximize the performance is analyzed. As a conclusion, it is beneficial to have more antennas at the base station and the appropriate tilt angle and the number of users to obtain the optimal achievable sum rate.

References

[1] D. Gesbert, M, Kountouris, R. W. Heath Jr., C. -B. Chae, and T. Salzer, "Shifting the MIMO paradigm," *IEEE Signal Processing Magazine*, vol. 24, no. 5, pp. 36-46, Sept.2007. Article (CrossRef Link)

[2] C. Diao, W. Xu, M. Chen, and B. Wu, "Outage probability analysis of multiuser MISO system exploiting joint spatial diversity and multiuser diversity with outdated feedback," *KSII Transactions on Internet and Information Systems*, vol. 5, no. 9, September, 2011. Article (CrossRef Link)

[3] H. Cao, Y. Lu, and J. Cai, "MMSE transmit optimization for multiuser multiple-input single-output broadcasting channels in cogitive radio networks," *KSII Transactions on Internet and Information Systems*, vol. 7, no. 9, September, 2013. Article (CrossRef Link)

[4] F. Gil, A. R. Claro, J. M. Ferreira, C. Pardelinha, and L. M. Correia, "A 3-D extrapolation model for base antennas' radiation patterns," *IEEE Transactions on Antennas and Propagation Magazine*, vol.43, no. 2, pp. 132-137, Apr., 2001. Article (CrossRef Link)

[5] F. Mikas and P. Pechac, "The 3-D approximation of antenna radiation patterns," in *Proc. of Inst. Electronics Engineering 12th International Conference Antennas Propagation*, ICAP, pp. 751-754, 2003. Article (CrossRef Link)

[6] M. Shafi, M. Zhang, A.L. Moustakas, P.J. Smith, A.F. Molisch, F. Tufvesson, S.H. Simom. "Polarized MIMO Channels in 3D: Models, Measurements and Mutual Information," *IEEE Journal on Selected Areas in Communications*. Vol. 24, pp 514 – 527, 2006. Article (CrossRef Link)

[7] T. G. Vasiliadis, A. G. Dimitriou, G. D. Sergiadis, "A Novel Technique for the Approximation of 3-D Antenna Radiation Patterns," *IEEE Transactions on Antennas and Progagation*, 53, July, 2005. Article (CrossRef Link)

[8] F. Gunnarsson, M. N. Johansson, A. Furuskar, M. Lundevall, A. Simonsson, C. Tidestav, and M. Blomgren, "Downtilted base station antennas - a simulation model proposal and impact on HSPA and LTE performance," in *Proc. of VTC 2008-Fall Vhicular Technology Conference IEEE 68th*, pp. 1-5, 2008. Article (CrossRef Link)

[9] F. Rusek, D. Persson, B. K. Lau, E. G. Larsson, O. Edfors, F. Tufvesson, and T. L. Marzetta, "Scaling up MIMO: Opportunities and Challenges with Very Large Arrays," *IEEE Signal Processing. Magazine*, Vol. 30, no. 1, pp. 40-60, Jan., 2013. Article (CrossRef Link)

[10] H. Gao, and R. Song, "Distributed compressive sensing based channel feedback scheme for massive antenna arrays," *KSII Transaction on Internet and Information Systems* vol. 8, no.1, Jan., 2014. Article (CrossRef Link)

[11] T. L. Marzetta, "Noncooperative cellular wireless with unlimited number of BS antennas," *IEEE Transactions Wireless Communication*, vol. 9, no. 11, pp. 3590-3600, Nov., 2010. Article (CrossRef Link)

[12] Y. Zhang, H. Long, Y. Peng, K Zheng, and W. Wang, "User-Oriented- and Spectral-Efficiency

Tradeoff for Wireless Networks," *KSII Transactions on Internet and Information Systems*, vol. 4, no. 3, February, 2013. Article (CrossRef Link)

[13] H. Q. Ngo, E. G. Larsson, and T. L. Marzetta, "Energy and Spectral Efficiency of Very Large Multiuser MIMO Systems," *IEEE Transactions Communication*, 2012, to be published. Article (CrossRef Link)

[14] J. Hoydis, S. ten Brink, and M. Debbah, "Massive MIMO in the UL/DL of cellular networks: How many antennas do we need?" *IEEE Journal on Selected Areas in Communications*, vol.31, no. 2, pp. 160-171, Feb., 2013. Article (CrossRef Link)

[15] M. -S. Alouini and A, J. Goldsmith, "Area spectral efficiency of cellular mobile radio systems," *IEEE Transactions Wireless Communication*, vol. 48, no. 4, pp. 1047-1066, Jul., 1999. Article (CrossRef Link)

[16] G. Rajamani and J. Kuriacose, "Effect of Non-uniform Traffic Distribution on Performance of a Cellular CDMA System," *International Conference on Personal Communications*, vol. 2, no. 1, pp. 598-602, Oct., 1997. Article (CrossRef Link)

[17] J. S. Thompson, P. M Grant, and B. Mulgrew, "The Effects of User Distribution on CDMA Antenna Array Receivers," *IEEE Signal Processing Workshop on Signal processing in Wireless Communications*, pp. 181-184, Apr., 1997. Article (CrossRef Link)

[18] T. Liu, J. Peng, X. F. Wang, J. Yang, and B. Guo, "Research on the Energy Hole Problem Based on Non-uniform Node Distribution for wireless Sensor Networks," *KSII Transactions on Internet and Information Systems*, vol. 6, no. 9, February, 2012. Article (CrossRef Link)

[19] M. Matthaiou, C. Zhong, M. R. McKay, T. Ratnarajah, "Sum Rate Analysis of ZF Receivers in Distributed MIMO Systems," *IEEE Journal on Selected Areas in Communications*, vol. 31, no. 2, pp. 180-191, February, 2013. Article (CrossRef Link)

[20] A. Muller, J. Hoydis, R.Couillet, and M. Debbah, "Optimal 3D Cell Planning: A Random Matrix Approach," *IEEE Global Communications Conference*, Anaheim, California, USA, 2012. Article (CrossRef Link)

[21] X. Li, L. Li, L. Xie, J. Jin, W. Wang, "Sum Rate Analysis of MU-MIMO with 3D Base Station Exploiting Elevation Features," submitted to *Journal of China Universities of Posts and Telecommunications*, 2014.

[22] M. K. Simon and M. S. Alouini, "Digital Communication Over Fading Channels," New York: Wiley, 2000. Article (CrossRef Link)

[23] N. Seifi, M. Coldrey, and M. Viberg, "Throughput Optimization for MISO Interference Channels via Coordinated User-Specific Tilting," *IEEE Communication Letters*, 2012. Article (CrossRef Link)

[24] A. M. Tulino and S. Verdu, Random Matrix Theory and Wireless Communications. 1st ed. http://www.nowpublisher.com/: Now (an Internet-Based publisher), the essence of Knowledge: *Foundations and Trends in Communications and Information Theory*, 2004. Article (CrossRef Link)

Xingwang Li received the B.Sc. degree in communication engineering from Henan Polytechnic University, China, in 2007 and M.S. degree in the National Key Laboratory of Science and Technology on Communications at University of Electronic Science and Technology of China, in 2010. From 2012 to now, he is working toward his Ph.D. in the State Key Laboratory of Networking and Switching Technology at Beijing University of Posts and Telecommunications (BUPT). His research interests include MIMO for wireless communication, massive MIMO, 3D MIMO, cooperative communication, and performance analysis of fading channels.

Lihua Li received her doctor degree in 2004 at Beijing University of Posts and Telecommunications (BUPT). She is currently an associate professor in BUPT. She had been a short-term visiting scholar at Brunel University in UK in 2006. And she visited the University of Oulu from August 2010 to August 2011. Her research focuses on wideband mobile communication technologies including MIMO, link adaptation, cooperative transmission technologies etc. relating to new generation mobile communication systems such as LTE and IMT-Advanced. She has published 63 papers in international and domestic journals and academic conferences, and 5 books. She has applied 20 national invention patents and one international patent. She was selected and funded as one of the New Century Excellent Talents by the Chinese Ministry of Education in 2008. She has won the second prize of China State Technological Invention Award (the 1st level award in China) in 2008 and the first prize of China Institute of Communications Science and Technology Award in 2006 for her research achievements of “Wideband Wireless Mobile TDD-OFDM-MIMO Technologies”. She has served as a group leader in 3GPP LTE RAN1 standardization work on behalf of BUPT in 2005, when she submitted more than 20 relevant proposals to 3GPP LTE and 7 of them were accepted. She has taken part in China IMT-Advanced technology work group since 2007. And so far she has submitted 33 relevant proposals，15 of which were accepted.

Ling Xie received the B.Sc. degree in the major of Telecommunication Engineering with Management from Beijing University of Posts and Telecommunications (BUPT), China, in 2012. From 2012 to now, she is studying in the State Key Laboratory of Networking and Switching Technology of BUPT for her master degree. Her research mainly focuses on 3D MIMO, massive MIMO, and transceiver designs for new generation wireless communication.